

THE SHORT RANGE WAKEFIELDS OF THE TRAVELING WAVE AND STANDING WAVE X-BAND LINEARIZER OF FERMI@ELETTRA FEL: A COMPARATIVE STUDY

M. El Ashmawy, G. D'Auria, Sincrotrone Trieste ELETTRA, Italy.

Abstract

In most of the Linac based 4th Generation Light Sources now under development (e.g. FERMI@ELETTRA [1]), a short accelerating structure operating at higher harmonics (i.e. X-band, 12 GHz), is adopted to linearize the beam's longitudinal phase space [2]. This structure could be either travelling wave (TW) or standing wave (SW) type. As it is well known, each one of such structures has its own advantages and drawbacks in terms of RF properties but there is a lack of information about the wake fields of each type compared to the other. In this paper an overall comparison, from the wakefields point of view, of two different X-band structures will be carried out. The purpose is to evaluate quantitatively the longitudinal and transverse wake functions of the structures, determining their relevant wake integrals, such as the average value of energy loss, rms energy spread, kick factor and kick spread.

INTRODUCTION

The accelerating structure type (SW or TW) is usually chosen and optimized according to specific needs for some application where each type has its advantages rather than the other. However, in some applications, like linearizing the beam's longitudinal phase space in FEL facilities, the linac type is not crucial issue and preference is mainly decided based on its RF properties. However, for each type structures there is a lack of knowledge about the influence of the wake fields on the beam quality if they used in FEL where minimizing/mitigating the wakefields is mandatory to maintain the beam quality. Accordingly, we studied two TW and SW structures from the single bunch short wake-fields point of view as a further step in deciding the X-band linearizer type in FELs. As already pointed out this is done only from wakefields point of view. Figure 1 shows very well known two optimized structures used in this study; the constant impedance $2\pi/3$ TW and the on-axis coupling $\pi/2$ SW structures have been chosen as representatives of the travelling wave and standing wave linacs respectively.

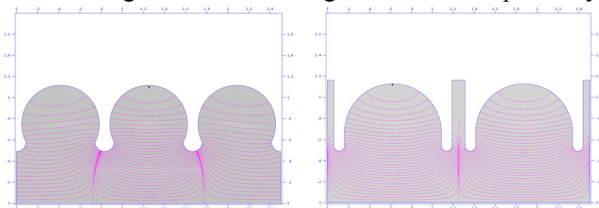


Figure 1. Left: 3 similar rounded cells with sphere-like nose of constant impedance $2\pi/3$ TW X-band structure. Right: 4 cells (2 short coupling cells + 2 long accelerating cells) of electrically coupled $\pi/2$ SW X-band structure.

* mostafa.ashmawy@lycos.com

Two main parameters are fixed in both structures for meaningful comparison; namely: the length has been chosen to be 0.6 m and the iris radius is set to 0.49 cm. SUPERFISH [3] has been used to optimize both linacs.

SINGLE BUNCH LONGITUDINAL WAKES

Longitudinal Wake Functions of TW&SW Linacs

The longitudinal wake fields of Gaussian bunch with different rms lengths (100 - 1000 μm) are simulated numerically using ABCI code [4] as shown in Fig. 2. The longitudinal wake function in each structure is found by fitting the common envelope function that the longitudinal wakefields of all bunch lengths tend to follow after certain distance from the bunch center as indicated by black dashed line in Fig. 2 (up). The longitudinal wake functions of TW and SW structures are expressed by equations 1 and 2 respectively:

$$(w_{||})_{TW} = -61.8 z^{-0.2464} + 38575 z \quad (1)$$

$$(w_{||})_{SW} = 3726 z^{0.2245} - 1119.96 z \quad (2)$$

Such wake functions have been used to calculate analytically the longitudinal wake potentials for both structures; Figure 2 (down) shows the analytical longitudinal wake potentials in comparison with those of ABCI. It is very evident that equations 1 and 2 approximate very well the wake functions of TW and SW structures respectively.

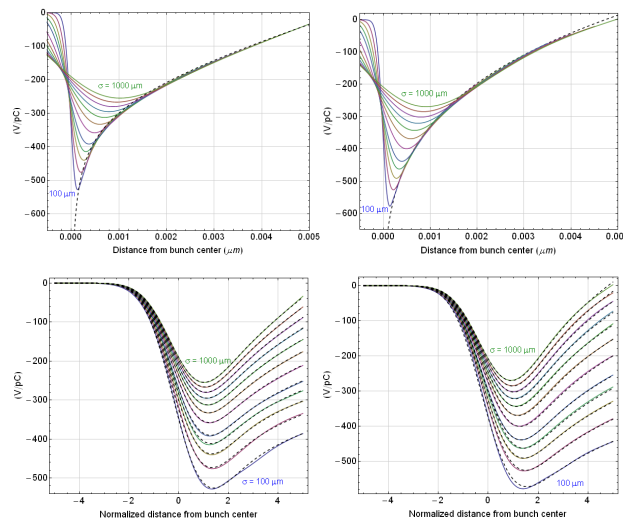


Figure 2: UP: longitudinal wake potentials (solid lines) and the relevant fitted wake functions (black dashed) for the TW (left) and SW (right) structures. Down: the numerical (solid lines) and the analytical ((black dashed) wake potentials of the TW (left) and SW (right) structures.

The validity and accuracy of such equations will be confirmed in the following subsection during the evaluation of the wake integrals. It is worthy to note that both longitudinal wake functions of both structures, represented by equations 1 and 2, could not be represented by the analytical approximation suggested in Ref. [5]; this is because the structures under study in this paper have different geometry than that used in the ref. [5], specially the SW structure.

Longitudinal Wake Integrals

The longitudinal wake integrals are known as the longitudinal loss factor and energy spread induced to the electron bunch due to the longitudinal wakefields and both are defined by equations 3 and 4 respectively.

$$K_{//} = \int_{-\infty}^{\infty} \lambda(s) W_{//}(s) ds \quad (3)$$

$$E_{//} = \sqrt{\int_{-\infty}^{\infty} \lambda(s) [W_{//}(s) - K_{//}]^2 ds} \quad (4)$$

Here $W_{//}$ is the longitudinal wake potential obtained by the convolution of the charge distribution function $\lambda(s)$ with the longitudinal wake function represented by equations 1 and 2. Figure 3 (up) represents both the numerical loss factor and energy spread in comparison with those obtained analytically by equations 3 and 4 for TW (left) and SW (right) structures. The analytical results agree very well with the numerical ones proving the validity and correctness of the longitudinal wake functions obtained previously. Figure 3 (down) represents a comparison between the numerical loss factor and energy spread for both the SW and TW structures (left) and their ratios (right).

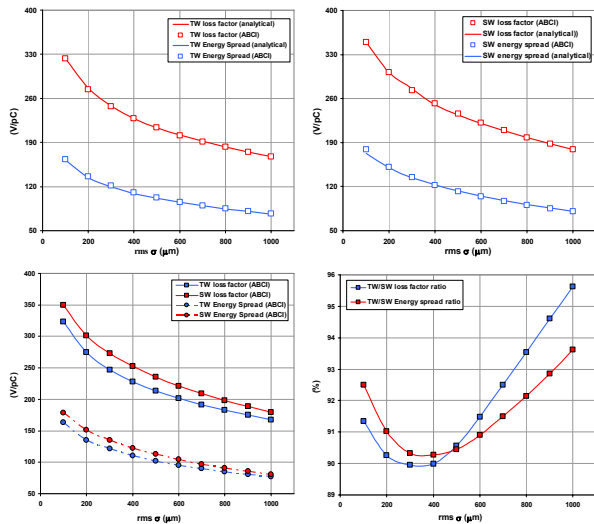


Figure 3: Up: numerical (squares) versus analytical (lines) loss factor (red) and energy spread (blue) for TW (left) and SW (right). Down: a comparison (left) of loss factors (lines) and energy spreads (dashed lines) of TW (blue) and SW (red); the right figure is for the TW/SW loss factor (blue) and energy spread (red) ratios.

The figure shows, generally, that the energy lost by a bunch of 1 pC charge in SW structure and consequently the energy spread are higher than those of TW case. However, the differences in the wake integrals are not fixed along all bunch lengths where the maximum difference is observed at intermediate bunch lengths ($\sigma \approx 250$ - $500 \mu\text{m}$).

SINGLE BUNCH TRANSVERSE WAKES

Transverse Wake Functions of TW&SW Linacs

By the same manner, the transverse wake fields of Gaussian bunch with different rms bunch lengths (200: 1000 μm) are simulated numerically using ABCI code as shown in Fig. 4. Also, the transverse wake function in each structure is found by fitting the common envelope function that the transverse wakefields of all bunch lengths tend to follow after certain distance from the bunch center as indicated by black dashed line in Fig. 4 (up). The transverse wake functions of TW and SW linacs are expressed by equations 3 and 4 respectively:

$$(w_T)_{TW} = 2.63 \cdot 10^6 e^{-256z} + 2.62 \cdot 10^6 e^{-268z} \quad (5)$$

$$(w_T)_{SW} = 2.74 \cdot 10^6 e^{-371z} + 2.74 \cdot 10^6 e^{-331z} \quad (6)$$

Such wake functions have been used to calculate analytically the transverse wake potentials of both structures; Figure 4 (down) shows the analytical longitudinal wake potentials in comparison with those obtained by ABCI. The results show that both equations 5 and 6 are very good analytical approximations of the transverse wake functions of the TW and SW structures respectively. Again, such wake functions could not be fit by the analytical approximation suggested in Ref. [5] for the same reasons aforementioned in longitudinal case.

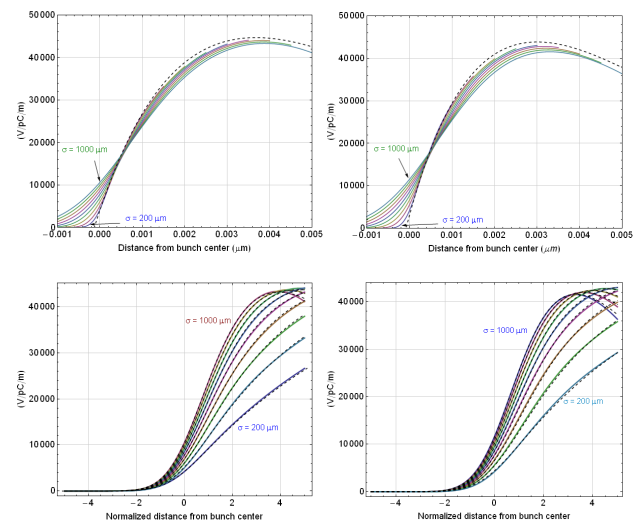


Figure 4: UP: transverse wake potentials (solid lines) and the relevant fitted wake functions (black dashed) for the TW (left) and SW (right) structures. Down: the numerical (solid lines) and the analytical ((black dashed) wake potentials of the TW (left) and SW (right) structures.

Transverse Wake Integrals

The transverse wake integrals are known as the transverse kick factor and kick spread induced to the electron bunch due to the transverse wakefields and both are defined by equations 7 and 8 respectively.

$$K_{\perp} = \int_{-\infty}^{\infty} \lambda(s) W_{\perp}(s) ds \quad (7)$$

$$E_{\perp} = \sqrt{\int_{-\infty}^{\infty} \lambda(s) [W_{\perp}(s) - K_{\perp}]^2 ds} \quad (8)$$

Here W_{\perp} is the transverse wake potential obtained by the convolution of the charge distribution function $\lambda(s)$ with the transverse wake function given by equations 5 and 6. Figure 5 (up) represents both the numerical kick factor and kick spread in comparison with those obtained analytically by equations 7 and 8 for TW (left) and SW (right) structures. The analytical results are in good coincidence with the ABCI data which reflect the validity and correctness of the transverse wake functions obtained previously. Figure 5 (down) represents a comparison between the ABCI numerical kick factor and energy spread for both the SW and TW structures (left) and their ratios (right).

As in the longitudinal wake case, the figure shows that the transverse kick factor in a bunch of 1 pC charge in SW structure and the associated induced kick spread are higher than those of TW case at all bunch lengths. Also, the differences in the transverse wake integrals of SW and TW linacs are not fixed along all bunch lengths where the maximum difference is almost observed at the same rms bunch lengths aforementioned in longitudinal wake case i.e. ($\sigma \approx 250$ - $500 \mu\text{m}$).

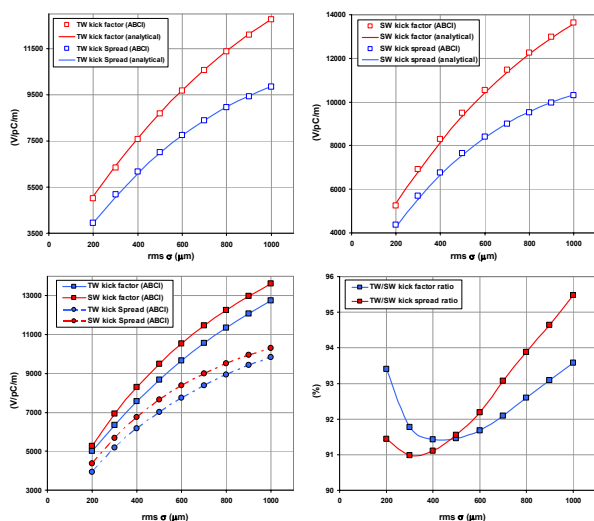


Figure 5: Up: numerical (squares) versus analytical (lines) kick factor (red) and energy spread (blue) for TW (left) and SW (right) structures. Down: a comparison (left) of kick factors (lines) and kick spreads (dashed lines) of TW (blue) and SW (red); the right figure is for the TW/SW kick factor (blue) and kick spread (red) ratios.

SUMMARY AND CONCLUSION

The short range transverse and longitudinal wakefields of different bunch lengths have been presented in both SW and TW X-band structures with length of 0.6 m and iris radius of 0.49 cm. ABCI code has been used to evaluate the numerical results of wakefields from which we extracted the longitudinal and transverse wake functions of both structures. The wake functions are then used to evaluate the relevant wake integrals: loss factor, energy spread, kick factor and kick spread in both structures and all are then brought to inter comparison. The comparison indicates that all of the wake integrals in SW structure are generally higher than those of TW structure, this is mainly attributed to the number of irises per one wave length in each structure where there are 4 irises in SW structure while there are 3 irises in TW one. However, the wake integrals of SW structure show maximums about 8-10% with respect to the TW structure at certain bunch length range ($\sigma \approx 200$ - $500 \mu\text{m}$); fore and aft these range the wake integrals of both linacs start to go close to each other. Accordingly, since the effect of the structure type on the beam quality is not the same for all bunch lengths, choice of structure type for linearizing the longitudinal beam phase space could be made on the basis of total wakefield budget available for the beam before the compression process on one hand and according to the rms bunch length at the X-band linac. The total bunch charge and energy are also very important factors for precise assessments of wakefields effect on the beam quality where the “higher energy” / “lower charge” the lower energy spread and deflection angles induced to the electron bunch.

ACKNOWLEDGEMENT

The authors undertook this work with the support of the ICTP programme for Training and Research in Italian Laboratories, Trieste, Italy

REFERENCES

- [1] FERMI@Elettra Conceptual Design Report.
- [2] P. Emma “X-Band RF Harmonic Compensation for Linear Bunch Compression in the LCLS” SLAC-TN-05-004, LCLS-TN-01-1, (2001).
- [3] K. Halbach and R. F. Holsinger, “SUPERFISH – A Computer Program for Evaluation of RF Cavities with Cylindrical Symmetry,” Particle Accelerators 7 pp. 213-222, (1976).
- [4] ABCI website: <http://abci.kek.jp/abci.htm>.
- [5] K. Bane, “Short-range dipole wakefields in accelerating structures for the NLC”, SLAC-PUB-9663, LCC-0116, (2003).